Development of a Structure-based Computational Simulation to Optimize the Blocking Efficacy of Pro-antibodies

Bo-Cheng Huang
National Sun Yat-sen University
Yun-Chi Lu
Kaohsiung Medical University
Jun-Min Liao
Kaohsiung Medical University
Hui-Ju Liu
Kaohsiung Medical University
Shih-Ting Hong
Kaohsiung Medical University
Yuan-Chin Hsieh
I-Shou University
Chih-Hung Chuang
Kaohsiung Medical University
Huei-Jen Chen
Kaohsiung Medical University
Tzu-Yi Liao
Kaohsiung Medical University
Kai-Wen Ho
Kaohsiung Medical University
Yeng-Tseng Wang
Kaohsiung Medical University
Tian-Lu Cheng (tlcheng5024@gmail.com)
Institute of Biomedical Sciences, National Sun Yat-Sen University, Kaohsiung, Taiwan
https://orcid.org/0000-0002-7263-2766

Research

Keywords: Pro-antibody, Ab lock, Spatial hindrance, Computational simulation, Cover rate, Blocking ability, anti-PD-1 antibody, anti-IL-1β antibody, anti-CTLA-4 antibody, anti-TNFα antibody

Posted Date: December 18th, 2020

DOI: https://doi.org/10.21203/rs.3.rs-128660/v1

Abstract

Background: The on-target toxicity of monoclonal antibodies (Abs) is mainly due to the fact that Abs cannot distinguish target antigens (Ags) expressed in disease regions from those in normal tissues during systemic administration. In order to overcome this issue, we “copied” an autologous Ab hinge as an “Ab lock” and “pasted” it on the binding site of the Ab by connecting a protease substrate and linker in between to generate a pro-Ab, which can be specifically activated in the disease region to enhance Ab selectivity and reduce side effects. Previously, we reported that 70% of pro-Abs can achieve more than 100-fold blocking ability compared to the parental Abs. However, 30% of pro-Abs do not have such efficient blocking ability. This is because the same Ab lock linker cannot be applied to every Ab due to the differences in the complementarity-determining region (CDR) loops. Here we designed a method which uses structure-based computational simulation (MSCS) to optimize the blocking ability of the Ab lock for all Ab drugs. MSCS can precisely adjust the amino acid composition of the linker between the Ab lock and Ab drug with the assistance of molecular simulation.

Results: We selected αPD-1, αIL-1β, αCTLA-4 and αTNFα Ab as models and attached the Ab lock with various linkers (L1 to L7) to form pro-Abs by MSCS, respectively. The resulting cover rates of the Ab lock with various linkers compared to the Ab drug were in the range 28.33%-42.33%. The recombinant pro-Abs were generated by MSCS prediction in order to verify the application of molecular simulation for pro-Ab development. The binding kinetics effective concentration (EC-50) for αPD-1 (200-250-fold), αIL-1β (152-186-fold), αCTLA-4 (68-150-fold) and αTNFα Ab (20-123-fold) were presented as the blocking ability of pro-Ab compared to the Ab drug. Further, there was a positive correlation between cover rate and blocking ability of all pro-Ab candidates.

Conclusions: The results suggested that MSCS was able to predict the Ab lock linker most suitable for application to αPD-1, αIL-1β, αCTLA-4 and αTNFα Ab to form pro-Abs efficiently. The success of MSCS in optimizing the pro-Ab can aid the development of next-generation pro-Ab drugs to significantly improve Ab-based therapies and thus patients’ quality of life.

Introduction

Monoclonal antibodies (Abs) have been regarded as potential therapeutics due to their antigen (Ag) specificity that can be applied to multiple diseases, such as malignant cancers[1-4], chronic diseases[5] and autoimmune diseases[6, 7]. However, the targeted Ags are not only expressed in the disease area but also in the healthy region, causing unexpected on-target toxicity during systemic over-activation.[8] Neutralization of the targeted Ag can also reduce therapeutic efficacy or even terminate drug treatment. For example, previous studies have reported that the immune checkpoint drug antagonists: Ipilimumab (αCTLA-4 Ab) and Nivolumab (αPD-1 Ab) may systemically target CTLA-4/ PD-1 and over-activate immune cells, causing immune-related adverse events such as hepatitis, colitis, thyroid disorders, and even paralysis.[9-11] On the other hand, the Ab drugs for rheumatoid arthritis (RA), Infliximab and Adalimumab (αTNFα Ab) have been reported to reduce pathological inflammation and inhibit RA

progression through targeting TNFα, which modulates host defense and tumor growth. Systemic neutralization of TNFα may lead to severe infections, reactivation of viral infections (hepatitis or herpes zoster), and raise the risk of malignancy.[12-14] Canakinumab (αIL-1β Ab) is an IL-1β blocker for patients who suffer from associated periodic syndromes (CAPS), IL-1β plays a role in resisting inflammation and regulating immune response, which by systemic neutralization causes on-targeted toxicities such as increasing risk of pneumonia, bone and joint infections.[15] To sum up, the U.S. Food and Drug Administration (FDA) has indicated that most therapeutic Abs have on-target toxicity issues and therefore limits their application.[8, 16, 17] Hence, enhancement of Ab selectivity and reduction of side effects are necessary if Ab-based therapies are to be effectively used in the clinic.

In our previous research, we developed a spatial hindrance-based “Ab lock” to generate pro-Abs which can increase Ab selectivity and safety. We “copied” the autologous Ab hinge as an “Ab lock” and “pasted” it onto the binding site of the Ab by connecting a protease substrate and linker in between to generate a pro-Ab.[18] Once the Ab lock is cleaved from the pro-Ab by a protease expressed at the disease region, the Ab is expected to have restored binding ability and neutralize its target Ag. In our previous study, we generated pro-Infliximab which can be selectively activated by MMP-2/9 only at the RA region. The Ab lock significantly inhibits TNFα binding of pro-Infliximab by 395-fold compared with Infliximab, and MMP-2/9 protease treatment to pro-Infliximab can completely restore the neutralization of TNFα. Further, pro-Infliximab not only showed equivalent therapeutic efficacy to Infliximab but also maintained immunity against *Listeria* infection in the RA mouse model, which led to a 71% survival rate compared to 0% of the Infliximab treatment group, indicating that pro-Abs can enhance Ab selectivity and reduce side effects.[19] Our previous results showed that by using the concept of “copy and paste”, we transformed almost 70% of therapeutic Abs into pro-Abs and achieved over 100-fold blocking ability compared to the parental Abs. Hence, this strategy could be further applied to develop customized pro-Abs. However, 30% of pro-Abs did not achieve the blocking ability to even 50-fold compared to parental Abs. The reason for the low blocking ability is that there are distinct differences among the complementarity-determining region (CDR) loop of each Ab,[20, 21] so the identical linker of the Ab lock cannot be applied to every Ab. In order to overcome this issue, it is essential to design a method to predict and optimize the Ab lock with a suitable linker for each Ab.

Here we designed a method using structure-based computational simulation (MSCS) to predict the cover rate of the pro-Ab in order to select a suitable linker for the Ab lock applied to different Ab drugs. We precisely extended or shortened the length of the amino acid composition to form linkers (L1, L2, L3, L4, L5, L6 and L7) between the Ab lock and Ab drug. Next, we predicted pro-Abs with each Ab lock linker using Amber and Discovery Studio software to simulate and calculate the cover rate of the Ab lock to each CDR residue. The cover rate was determined by a homemade program which analyzes the trajectories and calculates the frequency if any atom of hinge, linker or substrate above 120° and 4Å of any atom of CDR amino acids. In order to confirm the accuracy of the MSCS, we selected four Ab drugs: αPD-1, αIL-1β, αCTLA-4, and αTNFα Ab as models to simulate pro-Abs with the following Ab lock linkers: pro-αPD-1 Ab (L2 and L3), pro-αIL-1β Ab (L3 and L4), pro-αCTLA-4 Ab (L1 and L2) and pro-αTNFα Ab (L5, L6, and L7), and calculated their cover rate, respectively. Then, we generated the recombinant pro-Abs and

evaluated the blocking ability using biological assays. Finally, we analyzed the correlation between the blocking ability and the cover rate to verify the accuracy of the MSCS. If it is possible to efficiently transform any Ab into a pro-Ab using MSCS, the development of pro-Ab will be facilitated and Ab therapeutic efficacy will be improved. In addition, serious side effects can be avoided, thereby improving patients' quality of life.

Materials And Methods

Cells

The Expi293F cells (Thermo Fisher Scientific, Waltham, MA, USA) were cultured in Expi293 Expression Medium (Thermo Fisher Scientific, catalog A1435102) at 37°C in a humidified atmosphere of 8% CO_2.

Pro-Ab construction, expression, and purification

The complementary DNA coding for the heavy and light chains of the pro-Abs and Abs were cloned based on the Ab (αCTLA-4, αPD-1, αIL-1β and αTNFα) DNA construct through assembly PCR. Human IgG1 hinge sequences were obtained from the National Center for Biotechnology Information. The hinge-encoding sequences (EPKSCDKTHTCPPCP), linkers (L1-VL: VNGGGGS-GPLGVR-AAQPA/ L1-VH: GGRGGGGS-GPLGVR-RS; L2-VL: VN-GPLGVR-AAQPA/ L2-VH: GGR-GPLGVR-PGRS; L3-VL: GGGGS-GPLGVR-AAQPA/ L3-VH: VNAAAGGGGS-GPLGVR-RS; L4-VL: -GPLGVR-AAQPA/ L4-VH: VNAAA-GPLGVR-PGRS; L5-VL: GGGGS-GPLGVR-GGGGS/ L5-VH: GGGGS-GPLGVR-GGGGS; L6-VL: GGGGS-GPLGVR-GGGFS/ L6-VH: GGGGS-GPLGVR-GGGFS; L7-VL: -GPLGVR-GGGDS/ L7-VH: -GPLGVR-GGGDS), and MMP-2/9 substrate-encoding sequences (GPLGVR) were introduced upstream of the light chain and heavy chain to generate pro-Abs (pro-αCTLA-4, pro-αPD-1, pro-αIL-1β and pro-αTNFα). All Ab or pro-Ab production was generated through the Expi293 Expression System (Thermo Fisher Scientific,Waltham, MA, USA) and was purified using Protein A-Sepharose (GE Healthcare, Milwaukee, WI, USA).

Computational structure predictions for pro-Abs

The structure of the antibodies was extracted from the crystal structure from the Protein Data Bank[22] or homology modeling if the crystal structure is not solved. Only Fv segments were used in the simulations. The IgG1 hinges were built by homology modeling. These hinges were combined with linkers and MMP-2/9 substrate segments (GPLGVR), and then attached to the N-terminal of the Ab to construct pro-Ab structures. The combined structures were built using Discovery Studio (San Diego, CA, USA), and then further refined by energy minimizations and heating, followed by 100 ns GaMD simulations[23] at 310K using AMBER[24] with the generalized Born solvent model (GB/SA)[25]. The cover rate was determined using a homemade program which analyzes the trajectories and calculates the frequency if any atom of the hinge, linker or substrate reaches above 120° and 4Å for any atom of the CDR amino acids.

Comparison of the binding ability of pro-Abs with or without MMP-2/9 treatment

To determine the binding kinetics effective concentration (EC-50) of pro-Abs (pro-αCTLA-4, pro-αPD-1, pro-αIL-1β and pro-αTNFα Ab) and Abs (αCTLA-4, αPD-1, αIL-1β and αTNFα Ab), the recombinant Ag- CTLA-4, PD-1, IL-1β and TNFα were coated onto 96-well plates and blocked with 5% skim milk. The Pro-Ab or Ab were added onto the plates at the given concentrations (αCTLA-4 and pro-αCTLA-4 Abs: 107.4-0.0138 nM, 6-fold serial dilutions; αPD-1 and pro-αPD-1 Abs: 4000-0.004 nM, 10-fold serial dilutions; αIL-1β and pro-αIL-1β Abs: 1440-0.0014 nM, 10-fold serial dilutions; αTNFα and pro-αTNFα Ab: 500-0.0005 nM, 10-fold serial dilutions) for 1 h at RT. After washing, the wells were incubated with HRP-goat anti human IgG Fcγ Ab for 1 h at RT, and detection was performed by the addition of ABTS containing 30% H_2O_2 (Sigma-Aldrich). The binding ability was quantified through absorbance detection at 405 nm.

Results

Prediction of the structure of pro-Ab candidates with different linkers to analyze the cover rate of the Ab lock

To construct the structures of the pro-Abs, we first obtained the crystal structure of the Ab Fab fragment from the protein data bank. The IgG1 hinge (Ab lock) was built by homology modeling, and attached to the Ab Fab fragment through protease substrate and linker to generate pro-Ab Fab structure. In order to select a suitable linker to generate a pro-Ab with high blocking efficiency, we designed a method which uses structure-based computational simulation (MSCS) to predict the cover rate of the Ab lock with various linkers. The cover rate of the Ab lock was identified as the frequency of the appearance of the Ab lock above 4 Å within 120 degrees of each amino acid on the CDR loop **(Fig. 1)**. Here, we selected four Abs: αCTLA-4, αPD-1, αIL-1β and αTNFα Ab as candidates with various linkers for which the lengths were extended or shortened between the Ab lock (EPKSCDKTHTCPPCP), MMP-2/9 substrate sequence (GPLGVR) and VL/H region **(Table 1)**. Further, these Ab locks with various kinds of linkers were observed to have a cover rate from 18.1% to 42.43% in four Ab drugs **(Table 2)**. The computer simulated results indicated that variation of the linker length and composition will lead to different cover rates of the Ab lock on the CDR region of the Ab.

Generation of the recombinant pro-Abs predicted by MSCS to confirm their blocking ability

We wanted to confirm the blocking ability of each pro-Ab with different Ab lock linker candidates, so we generated the pro-Abs and detected their binding kinetic by ELISA. We used gene engineering to generate the computer simulation selected-pro-Abs candidates of αCTLA-4 (L1 and L2), αPD-1 (L2 and L3), αIL-1β (L3 and L4) and αTNFα (L5, L6 and L7), respectively, and analyzed the blocking ability of the pro-Abs via Ag-base ELISA. The results of pro-αCTLA-4 Abs showed that the EC-50 of L1 Ab lock and L2 Ab lock had a 68-fold and 150-fold masking effect, respectively, compared to αCTLA-4 Ab alone **(Fig. 2A)**. As shown in Fig. 2B, the EC-50 of the L2 Ab lock had a 250-fold, and L3 had a 200-fold masking effect compared to αPD-1 Ab alone. The αIL-1β revealed that the EC-50 of the L3 Ab lock had a 152-fold, and L4 had a 186-fold masking effect compared to αIL-1β Ab alone **(Fig. 2C)**. And αTNFα showed that the EC-50 of the L5 Ab lock had a 31-fold, L6 Ab lock had a 38-fold, and L7 had a 39-fold masking effect compared to αTNFα

Ab alone **(Fig. 2D)**. These data indicated that among various linker candidates, the higher the cover rate the Ab lock had, the greater its blocking ability was. Also each Ab lock with different Ab lock linkers led to a distinct blocking ability **(Table 2)**. We successfully used this system to construct four kinds of pro-Abs, and the Ab locks with the computer simulation-selected linkers showed binding ability reduced by 31- to 200-fold compared to parental Ab drugs.

Analysis of the correlation between the cover rate and blocking ability of pro-Abs

To verify that the pro-Abs simulated by computer do not differ from the biological results, we analyzed the correlation between the computer simulated results-cover rate and blocking ability (**Fig. 3**). The candidates, which included αCTLA-4, αPD-1, αIL-1β and αTNFα Ab, showed positive correlations between the cover rate and blocking fold. The R^2 value of each pro-Ab we analyzed was 0.6435. These results indicated that the MSCS could predict the cover rate of the pro-Ab via computer modeling. By simulating the Ab lock and predicting the blocking ability of the pro-Ab by MSCS before generating it, we efficiently and accurately selected the optimal Ab lock candidate; therefore, customizing each Ab lock to different Ab drugs.

Discussion

We successfully designed a method which used structure-based computational simulation (MSCS) to efficiently select the most suitable linker for enhancing the blocking ability of various pro-Abs. We applied the concept of “copy and paste” to develop an autologous Ab lock which is connected by various linkers. Here we compared the cover rate of different Abs applied with different linkers, L1, L2, L3, L4, L5, L6 and L7, and connected them to αCTLA-4, αPD-1, αIL-1β and αTNFα Ab, respectively, as pro-Abs. We found that pro-αCTLA-4 with L2 linker can achieve higher cover rate (42.43%) compared to L1 linker (29.96%). Producing the recombinant pro-Abs mentioned above biologically to evaluate their blocking ability confirmed that the linker with a higher cover rate had better masking ability. Likewise, pro-αPD-1 with the L2 linker (41.19% of cover rate) had better masking ability (250-fold) compared to L3 linker (28.33% of cover rate, 200-fold). During the analysis we found that there was a positive correlation between the cover rate and masking ability, indicating our MSCS can select the Ab lock with the appropriate linker depending on different Ab drug characteristics to efficiently optimize pro-Abs. This way, scientists can easily apply the “copy and paste” concept to generate an efficient pro-Ab according to the MSCS. Using this method, pro-Abs can be more widely developed to enhance drug selectivity and reduce on-toxicity of Abs.

It is important to develop pro-Abs depending on the diversity of the CDR loop of each Ab. The structure motif of the CDR loop is a key to determining the difference in bio-activity of each Ab. For example, Regep and colleagues screened 1,779 structures and calculated that over 30% of CDR-H3 loops play a key role in the ability of the Ab to bind to the diverse spaces of potential Ags.[26] Avnir and colleagues developed an influenza hemagglutinin neutralizing Ab (anti-influenza A virus Ab) for which the major structure was achieved through two CDR-H2 loop anchor residues with the Phe54 residue having the dominant position.

[27] In addition to the CDR loop of the heavy chain, in some cases the CDR loop of light chain has also been reported to play the dominant role in Ag recognition. Van den Beucken and colleagues reported that they generated the affinity maturation of anti-streptavidin Ab fragments, R2H10 (3.2 nM) and R3B1 (5.5 nM), by yeast-display, then identified that mutation in CDR-L1 and CDR-L3 could improve the affinity 10.7-fold and 6.3-fold, respectively, compared to the starting Ab.[28] These examples indicate that the diversity of the CDR loop affects the characteristics of the Ab. Therefore, it is essential to customize the Ab lock for any Ab. Here we precisely adjusted the amino acid composition of the linker between the Ab lock and the Ab drug and predicted the most suitable linker via MSCS depending on variable CDRs. As a result, we confirmed that there is positive correlation between the cover rate simulated by MSCS and the blocking ability measured through biological assay. Our results not only showed the cover rate of the Ab lock with each linker but also the individual cover rate of each CDR loop. With MSCS, the linker could be adjusted in order to coordinate with the CDR loop of an Ab, which is the key dominant region. We thus designed a universal method-MSCS that can efficiently overcome the issue of poor pro-Ab blocking ability due to CDR diversity and generate better pro-Abs accurately.

Furthermore, blocking the binding of anti-idiotypic Ab (anti-Id Ab) and prolonging the serum half-life of Ab drug is desirable, because generation of anti-Id Abs have been reported to neutralize the activity of Ab drugs, thereby accelerating the clearance rate, reducing therapeutic effect of Ab drug, and even increasing the frequency of immune-mediated adverse effects.[29] Previous studies suggested that 28% Adalimumab-treated RA patients induced anti-Adalimumab Ab (> 97% are anti-Id Ab) during a 3-year treatment period. Anti-Adalimumab Ab reduces the serum concentration of Adalimumab and causes a 2-fold increase in treatment failure rate as compared with the anti-Adalimumab-negative Ab.[30] Davda also reported that Certolizumab pegol (anti-TNFa Fab' fragment bound to polyethylene glycol) induces anti-Id Ab generation to Certolizumab pegol in 8.1% RA patients at 24 weeks, thus, reducing the drug response (ACR20).[31] In addition, Weinblatt et al. indicated that a high incidence of anti-Id Ab (79%) was found following treatment with Alemtuzumab (anti-CD52 Ab) in patients with multiple sclerosis, and with reduced therapeutic efficacy.[4] These clinical findings indicated that preventing the interference effect of anti-Id Ab can solve many of the clinical problems of Ab drugs. Our team have demonstrated that the spatial hindrance–based Ab lock can prevent the response of anti-Id Ab to Infliximab (anti-I-Id Ab); the binding of the anti-I-Id Ab to pro-Infliximab was 108-fold weaker than that to Infliximab[19], and the Ab lock maintained the TNFa binding ability of pro-Infliximab which was pre-incubated with anti-Id Ab. In the future, we will be able to efficiently transform Abs into optimized pro-Abs to prevent the binding of anti-Id Ab using MSCS. The custom-designed linker can enhance the masking ability of Ab lock to cover the CDR region of each Ab, thereby restricting the generation of anti-Id Abs. We believe MSCS can generate safer pro-Abs and provide better therapeutic efficacy.

Last but not least, it is important to develop pro-Abs with changeable protease substrates depending on different protease-expressing diseases. Proteases are disease-specific diagnostic markers which offer a therapeutic index. Qu and colleagues reported high levels of expression of matrix metalloproteinase-9 (MMP-9) in breast cancer, which plays the role of tumor migration and invasion. MMP-9 belongs to the

family of Ca^{2+} and Zn^{2+} ion-dependent endopeptidases and has the ability to degrade extracellular matrix components, which indicates that MMP-9 is involved in tumorigenesis of breast cancer.[32] Choi and colleagues have reported proteases that are overexpressed in ovarian cancer, such as cathepsin D, which can promote tumor progression. Cathepsin D is localized in lysosomes, and is also detected at a high level in the area surrounding tumors which causes the invasion.[33] Duong and colleagues reported that osteoclasts express high levels of cathepsin K that can cause osteoporosis. Cathepsin K is a cysteine protease and has the ability to degrade the bone matrix and decrease bone mass, meaning cathepsin K may have the potential to be a new treatment target.[34] Many cases show that different diseases express several proteases. If we generate pro-Abs with different protease substrates, the distinct substrate will change the composition of the linker and the efficacy of the spatial-hindrance of the Ab lock, even affecting the blocking ability of the pro-Ab. In order to overcome this issue, we can utilize MSCS to calculate the cover rate of the pro-Ab with different protease substrates in the pro-Ab. MSCS will adjust the amino acid composition of the linker between the Ab lock and Ab drug with the assistance of molecular simulation, so that we can efficiently generate protease-independent pro-Abs, and thereby replace any protease as the substrate peptide of the pro-Ab depending on the disease. By MSCS, we can accelerate pro-Ab development which is dependent on different protease-expressing diseases.

In conclusion, we provide MSCS that can predict the cover rate of Ab locks to optimize and customize pro-Abs. MSCS has the following advantages: (1) it can adjust the cover rate of an Ab lock to the Ab binding site depending on the diversity of each CDR loop; (2) it can be utilized to predict the pro-Ab that may prevent anti-Id Ab neutralizing the Ab in the blood; (3) it can predict the pro-Abs that need to change the protease substrate for different protease-expressing diseases; (4) any scientist could easily apply MSCS to select the Ab lock with a most suitable linker to generate a pro-Ab. We expect that by using the MSCS strategy to develop pro-Abs it will be possible to accelerate the development of pro-Abs. In addition, it is possible to apply this system which make all Abs transform pro-Abs and simulate the cover rate of the inhibited domain. The development of pro-Abs can be expected to change the behavior of next-generation Abs and significantly improve Ab therapy.

Declarations

Ethics approval and consent to participate

Not applicable

Consent for publication

Not applicable

Availability of data and material

All data needed to evaluate the conclusions in the paper are present in the paper. Additional data related to this paper may be requested from the authors.

Competing interests

T.-L.C., C.-H.C.and Y.-C.L. are listed as inventors on patents [U.S. application number: 14/893,509] related to the technology described in this work. The other authors declare that they have no competing interests.

Funding

This work was supported by grants from the Ministry of Science and Technology, Taipei, Taiwan (MOST 107-2320-B-037-024 -MY3) (MOST 109-2320-B-037-010 -MY3); the National Health Research Institutes, Taiwan (NHRI-EX108-10729EI); Academia Sinica, Taiwan (AS-TP-107-L11); the Ministry of Education, Taiwan (108RSB0029); and the KMU-KMUH Co-Project of Key Research (KMU-DK109001), Research Foundation (KMU-DK109004) from Kaohsiung Medical University, Taiwan. This study is also supported partially by Kaohsiung Medical University Research Center Grant (Drug Development and Value Creation Research Center) (KMU-TC108A03).

Authors' contributions

B.-C.H. and Y.-C.L. contributed equally to this work. T.-L.C., B.-C.H., Y.-C.L., J.-M.L. and S.-T.H. designed the research, B.-C.H., Y.-C.L., S.-T.H., H.-J.C., T.-Y.L. and K.-W.H. performed the research and analyzed the data, B.-C.H., Y.-C.L. and H.-J.L. wrote the paper. Y.-C.H., C.-H.C., Y.-T.W. and T.-L.C assisted in eliminating problems during the experiments and provided suggestions for the manuscript.

Authors' information

[1]Institute of Biomedical Sciences, National Sun Yat-Sen University, Kaohsiung, Taiwan. [2]Department of Biomedical Science and Environmental Biology, Kaohsiung Medical University, Kaohsiung, Taiwan. [3]Drug Development and Value Creation Research Center, Kaohsiung Medical University, Kaohsiung, Taiwan. [4]Graduate Institute of Medicine, College of Medicine, Kaohsiung Medical University, Kaohsiung, Taiwan. [5]School of Medicine for International Students, I- Shou University, Kaohsiung, Taiwan. [6]Department of Medical Laboratory Science and Biotechnology, College of Health Sciences, Kaohsiung Medical University, Kaohsiung, Taiwan. [7]Department of Medical Research, Kaohsiung Medical University Hospital, Kaohsiung, Taiwan. [8]Department of Biochemistry, Kaohsiung Medical University, Kaohsiung, Taiwan.

Acknowledgements

Not applicable

References

1. Seidel, J.A., A. Otsuka, and K. Kabashima, *Anti-PD-1 and Anti-CTLA-4 Therapies in Cancer: Mechanisms of Action, Efficacy, and Limitations.* Frontiers in oncology, 2018. **8**: p. 86-86.

2. Qi, X., F. Li, Y. Wu, C. Cheng, P. Han, J. Wang, and X. Yang, *Optimization of 4-1BB antibody for cancer immunotherapy by balancing agonistic strength with FcγR affinity.* Nature Communications, 2019. **10**(1): p. 2141.
3. Fakih, M. and R. Wong, *Efficacy of the monoclonal antibody EGFR inhibitors for the treatment of metastatic colorectal cancer.* Current oncology (Toronto, Ont.), 2010. **17 Suppl 1**(Suppl 1): p. S3-S17.
4. Weinblatt, M.E., P.J. Maddison, K.J. Bulpitt, B.L. Hazleman, M.B. Urowitz, R.D. Sturrock, J.S. Coblyn, A.L. Maier, W.R. Spreen, V.K. Manna, and et al., *CAMPATH-1H, a humanized monoclonal antibody, in refractory rheumatoid arthritis. An intravenous dose-escalation study.* Arthritis Rheum, 1995. **38**(11): p. 1589-94.
5. Nixon, J., P. Newbold, T. Mustelin, G.P. Anderson, and R. Kolbeck, *Monoclonal antibody therapy for the treatment of asthma and chronic obstructive pulmonary disease with eosinophilic inflammation.* Pharmacology & Therapeutics, 2017. **169**: p. 57-77.
6. Cludts, I., F.R. Spinelli, F. Morello, J. Hockley, G. Valesini, and M. Wadhwa, *Anti-therapeutic antibodies and their clinical impact in patients treated with the TNF antagonist adalimumab.* Cytokine, 2017. **96**: p. 16-23.
7. Vermeire, S., M. Noman, G. Van Assche, F. Baert, K. Van Steen, N. Esters, S. Joossens, X. Bossuyt, and P. Rutgeerts, *Autoimmunity associated with anti-tumor necrosis factor α treatment in Crohn's disease: a prospective cohort study.* Gastroenterology, 2003. **125**(1): p. 32-39.
8. Hansel, T.T., H. Kropshofer, T. Singer, J.A. Mitchell, and A.J.T. George, *The safety and side effects of monoclonal antibodies.* Nature Reviews Drug Discovery, 2010. **9**(4): p. 325-338.
9. Kähler, K.C., J.C. Hassel, L. Heinzerling, C. Loquai, R. Mössner, S. Ugurel, L. Zimmer, and R. Gutzmer, *Management of side effects of immune checkpoint blockade by anti-CTLA-4 and anti-PD-1 antibodies in metastatic melanoma.* J Dtsch Dermatol Ges, 2016. **14**(7): p. 662-81.
10. Pol, J. and G. Kroemer, *Anti-CTLA-4 immunotherapy: uncoupling toxicity and efficacy.* Cell Research, 2018. **28**(5): p. 501-502.
11. Bajwa, R., A. Cheema, T. Khan, A. Amirpour, A. Paul, S. Chaughtai, S. Patel, T. Patel, J. Bramson, V. Gupta, M. Levitt, A. Asif, and M.A. Hossain, *Adverse Effects of Immune Checkpoint Inhibitors (Programmed Death-1 Inhibitors and Cytotoxic T-Lymphocyte-Associated Protein-4 Inhibitors): Results of a Retrospective Study.* Journal of clinical medicine research, 2019. **11**(4): p. 225-236.
12. Ferreira, I. and D. Isenberg, *Vaccines and biologics.* Annals of the Rheumatic Diseases, 2014. **73**(8): p. 1446.
13. Mercer, L.K., J. Askling, P. Raaschou, W.G. Dixon, L. Dreyer, M.L. Hetland, A. Strangfeld, A. Zink, X. Mariette, A. Finckh, H. Canhao, F. Iannone, J. Zavada, J. Morel, J.-E. Gottenberg, K.L. Hyrich, and J. Listing, *Risk of invasive melanoma in patients with rheumatoid arthritis treated with biologics: results from a collaborative project of 11 European biologic registers.* Annals of the Rheumatic Diseases, 2017. **76**(2): p. 386.
14. Mori, S. and S. Fujiyama, *Hepatitis B virus reactivation associated with antirheumatic therapy: Risk and prophylaxis recommendations.* World journal of gastroenterology, 2015. **21**(36): p. 10274-10289.

15. Bettiol, A., G. Lopalco, G. Emmi, L. Cantarini, M.L. Urban, A. Vitale, N. Denora, A. Lopalco, A. Cutrignelli, A. Lopedota, V. Venerito, M. Fornaro, A. Vannacci, D. Rigante, R. Cimaz, and F. Iannone, *Unveiling the Efficacy, Safety, and Tolerability of Anti-Interleukin-1 Treatment in Monogenic and Multifactorial Autoinflammatory Diseases.* International journal of molecular sciences, 2019. **20**(8): p. 1898.
16. Johnson, D.E., *Biotherapeutics: Challenges and Opportunities for Predictive Toxicology of Monoclonal Antibodies.* International journal of molecular sciences, 2018. **19**(11): p. 3685.
17. Chames, P., M. Van Regenmortel, E. Weiss, and D. Baty, *Therapeutic antibodies: successes, limitations and hopes for the future.* British journal of pharmacology, 2009. **157**(2): p. 220-233.
18. Lin, W.-W., Y.-C. Lu, C.-H. Chuang, and T.-L. Cheng, *Ab locks for improving the selectivity and safety of antibody drugs.* Journal of Biomedical Science, 2020. **27**(1): p. 76.
19. Lu, Y.-C., C.-H. Chuang, K.-H. Chuang, I.J. Chen, B.-C. Huang, W.-H. Lee, H.-E. Wang, J.-J. Li, Y.-A. Cheng, K.-W. Cheng, J.-Y. Wang, Y.-C. Hsieh, W.-W. Lin, and T.-L. Cheng, *Specific activation of pro-Infliximab enhances selectivity and safety of rheumatoid arthritis therapy.* PLOS Biology, 2019. **17**(6): p. e3000286.
20. Wong, W.K., J. Leem, and C.M. Deane, *Comparative Analysis of the CDR Loops of Antigen Receptors.* Frontiers in immunology, 2019. **10**: p. 2454-2454.
21. Sela-Culang, I., V. Kunik, and Y. Ofran, *The structural basis of antibody-antigen recognition.* Frontiers in immunology, 2013. **4**: p. 302-302.
22. Read, R.J., P.D. Adams, W.B. Arendall, 3rd, A.T. Brunger, P. Emsley, R.P. Joosten, G.J. Kleywegt, E.B. Krissinel, T. Lütteke, Z. Otwinowski, A. Perrakis, J.S. Richardson, W.H. Sheffler, J.L. Smith, I.J. Tickle, G. Vriend, and P.H. Zwart, *A new generation of crystallographic validation tools for the protein data bank.* Structure (London, England : 1993), 2011. **19**(10): p. 1395-1412.
23. Bhattarai, A. and Y. Miao, *Gaussian accelerated molecular dynamics for elucidation of drug pathways.* Expert opinion on drug discovery, 2018. **13**(11): p. 1055-1065.
24. Case, D.A., T.E. Cheatham, 3rd, T. Darden, H. Gohlke, R. Luo, K.M. Merz, Jr., A. Onufriev, C. Simmerling, B. Wang, and R.J. Woods, *The Amber biomolecular simulation programs.* Journal of computational chemistry, 2005. **26**(16): p. 1668-1688.
25. Onufriev, A.V. and D.A. Case, *Generalized Born Implicit Solvent Models for Biomolecules.* Annual review of biophysics, 2019. **48**: p. 275-296.
26. Regep, C., G. Georges, J. Shi, B. Popovic, and C.M. Deane, *The H3 loop of antibodies shows unique structural characteristics.* 2017. **85**(7): p. 1311-1318.
27. Lundin, A., R. Dijkman, T. Bergström, N. Kann, B. Adamiak, C. Hannoun, E. Kindler, H.R. Jónsdóttir, D. Muth, J. Kint, M. Forlenza, M.A. Müller, C. Drosten, V. Thiel, and E. Trybala, *Targeting membrane-bound viral RNA synthesis reveals potent inhibition of diverse coronaviruses including the middle East respiratory syndrome virus.* PLoS Pathog, 2014. **10**(5): p. e1004166.
28. van den Beucken, T., H. Pieters, M. Steukers, M. van der Vaart, R.C. Ladner, H.R. Hoogenboom, and S.E. Hufton, *Affinity maturation of Fab antibody fragments by fluorescent-activated cell sorting of*

yeast-displayed libraries. FEBS Lett, 2003. **546**(2-3): p. 288-94.

29. Godar, M., V. Morello, A. Sadi, A. Hultberg, N. De Jonge, C. Basilico, V. Hanssens, M. Saunders, B.N. Lambrecht, M. El Khattabi, H. de Haard, P. Michieli, and C. Blanchetot, *Dual anti-idiotypic purification of a novel, native-format biparatopic anti-MET antibody with improved in vitro and in vivo efficacy.* Scientific Reports, 2016. **6**(1): p. 31621.
30. Bartelds, G.M., C.L.M. Krieckaert, M.T. Nurmohamed, P.A. van Schouwenburg, W.F. Lems, J.W.R. Twisk, B.A.C. Dijkmans, L. Aarden, and G.J. Wolbink, *Development of Antidrug Antibodies Against Adalimumab and Association With Disease Activity and Treatment Failure During Long-term Follow-up.* JAMA, 2011. **305**(14): p. 1460-1468.
31. Ruiz Garcia, V., A. Burls, J.B. Cabello, P. Vela Casasempere, S. Bort-Marti, and J.A. Bernal, *Certolizumab pegol (CDP870) for rheumatoid arthritis in adults.* The Cochrane database of systematic reviews, 2017. **9**(9): p. CD007649-CD007649.
32. Qu, J., X. Zhao, X. Liu, Y. Sun, J. Wang, L. Liu, J. Wang, and J. Zhang, *Natriuretic peptide receptor a promotes breast cancer development by upregulating MMP9.* American journal of cancer research, 2019. **9**(7): p. 1415-1428.
33. Choi, K.Y., M. Swierczewska, S. Lee, and X. Chen, *Protease-Activated Drug Development.* Theranostics, 2012. **2**(2): p. 156-178.
34. Duong le, T., A.T. Leung, and B. Langdahl, *Cathepsin K Inhibition: A New Mechanism for the Treatment of Osteoporosis.* Calcif Tissue Int, 2016. **98**(4): p. 381-97.

Tables

Table 1. Design of various linkers that shorten or extend the amino acids to optimize the efficiency of pro-Ab using MSCS.

The pro-Abs consist of a hinge domain, MMP-2/9 substrate and linker. We selected seven linkers which had the composition of the sequence among hinge domain, MMP-2/9 substrate and Ab VH/VL altered. Each type is applied to optimize a different Ab by MSCS.

Name		IgG1 Hinge	Linker	MMP-2/9 substrate	Linker
L1	L:	EPKSCDKTHTCPPCP	VNGGGGS	GPLGVR	AAQPA~
	H:	EPKSCDKTHTCPPCP	GGRGGGGS	GPLGVR	RS~
L2	L:	EPKSCDKTHTCPPCP	VN	GPLGVR	AAQPA~
	H:	EPKSCDKTHTCPPCP	GGR	GPLGVR	PGRS~
L3	L:	EPKSCDKTHTCPPCP	GGGGS	GPLGVR	AAQPA~
	H:	EPKSCDKTHTCPPCP	VNAAAGGGGS	GPLGVR	RS~
L4	L:	EPKSCDKTHTCPPCP		GPLGVR	AAQPA~
	H:	EPKSCDKTHTCPPCP	VNAAA	GPLGVR	PGRS~
L5	L:	EPKSCDKTHTCPPCP	GGGGS	GPLGVR	GGGGS~
	H:	EPKSCDKTHTCPPCP	GGGGS	GPLGVR	GGGGS~
L6	L:	EPKSCDKTHTCPPCP	GGGGS	GPLGVR	GGGFS~
	H:	EPKSCDKTHTCPPCP	GGGGS	GPLGVR	GGGFS~
L7	L:	EPKSCDKTHTCPPCP		GPLGVR	GGGDS~
	H:	EPKSCDKTHTCPPCP		GPLGVR	GGGDS~

Table 2. Cover rate and blocking fold of various kinds of Ab lock on different Abs.

L1 and L2 were used as pro-Abs for αCTLA-4 Ab; L2 and L3 were for αPD-1 Ab; L3 and L4 were for αIL-1β Ab; and L5, L6 and L7 were for αTNFα Ab. The cover rate of each candidate was calculated by MSCS; the value of blocking fold was confirmed by ELISA assay.

	αCTLA-4		αPD-1		αIL-1β		αTNFα		
Types of linkers	L1	L2	L2	L3	L3	L4	L5	L6	L7
Cover rate %	29.96	42.43	41.19	28.33	37.18	38	18.1	22.28	23
Blocking fold	68	150	250	200	152	186	31	38	39

Figures

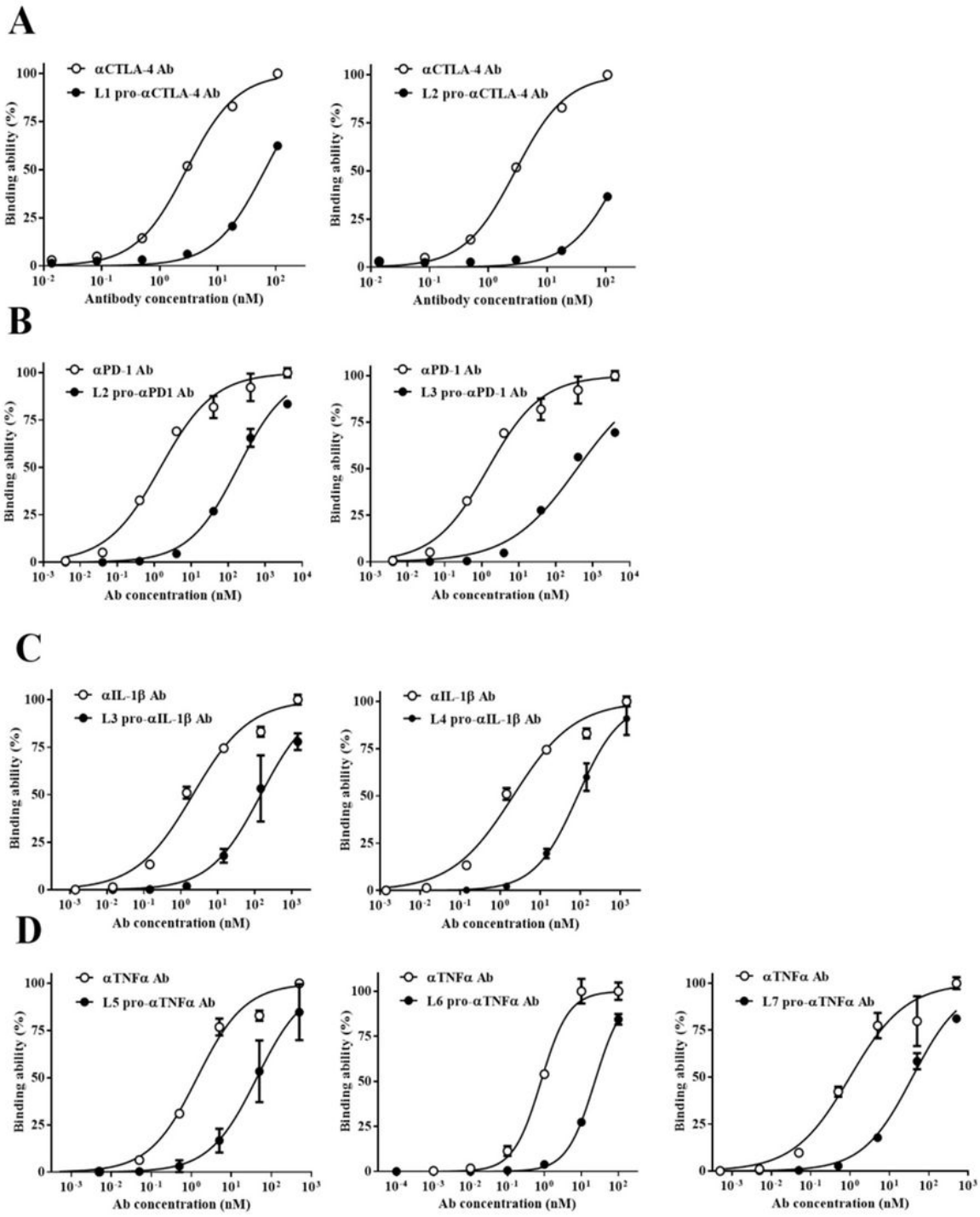

Figure 1

The blocking ability of each linker applied to different Abs. Pro-□CTLA-4 Ab with L1 and L2 linker (A), pro-□PD-1 Ab with L2 and L3 linker (B), pro-□IL-1β Ab with L3 and L4 linker (C), pro-□TNF□ Ab with L5, L6 and L7 linker (D) were added to 96-well plates pre-coated with recombinant Ag (CTLA-4, PD-1, IL-1β and TNF□). The binding ability of the parental Ab (●) and pro-Ab (●) were assessed by Ag-based ELISA. The values are mean ± SEM. Error bar: standard error of two determinations. Ab, antibody; CTLA-4, cytotoxic T-lymphocyte antigen 4; PD-1, programmed cell death protein 1; IL-1β, interleukin 1 beta; TNF□, tumor necrosis factor alpha; Ag, antigen.

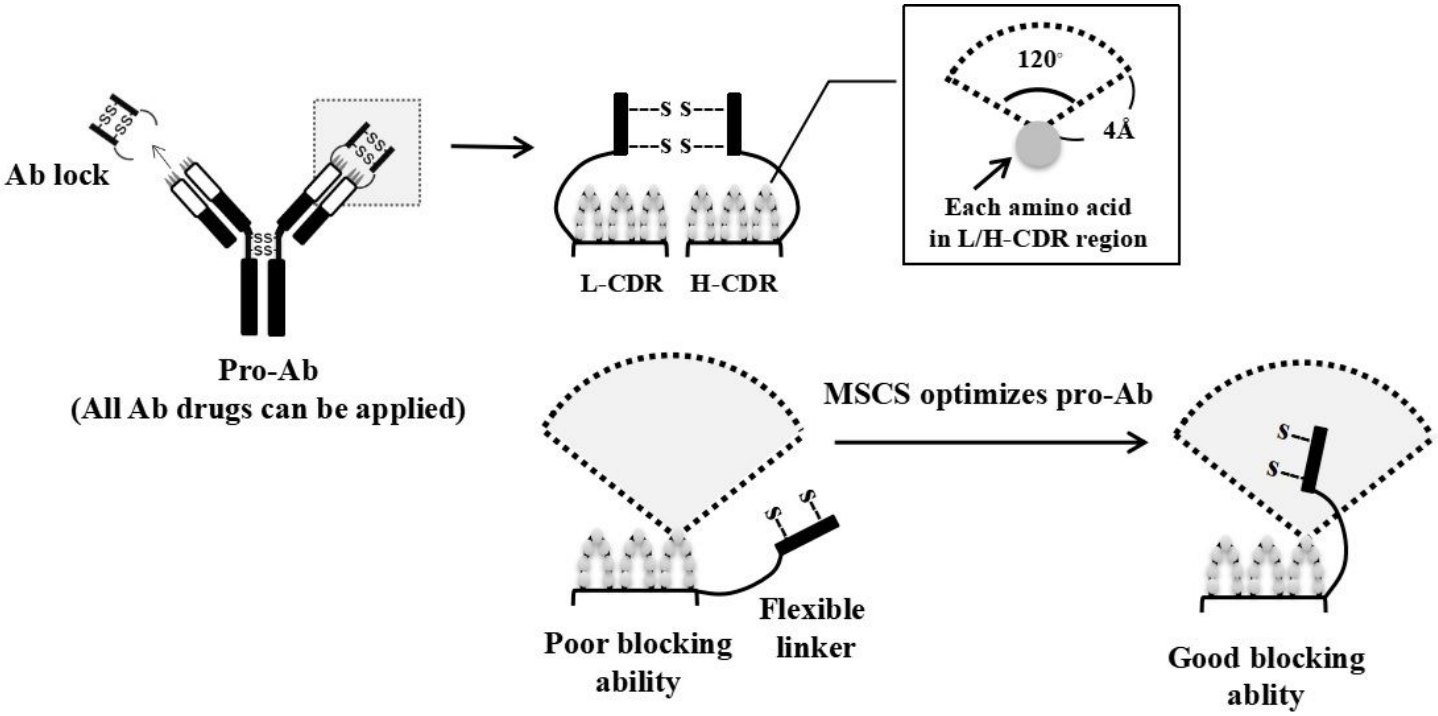

Figure 1

Schema of method of use of structure-based computational simulation (MSCS) used to optimize the blocking ability of Ab locks for Ab drugs. The pro-Ab blocks the binding ability of the CDR loop using an Ab lock. A pro-Ab can be applied to all Ab drugs. We designed a method which uses structure-based computational simulation (MSCS) to predict the cover rate of Ab locks with various linkers. The cover rate of the Ab locks was defined as the frequency of appearance of the Ab lock above 4 Å within 120 degrees of each amino acid on the CDR loop.

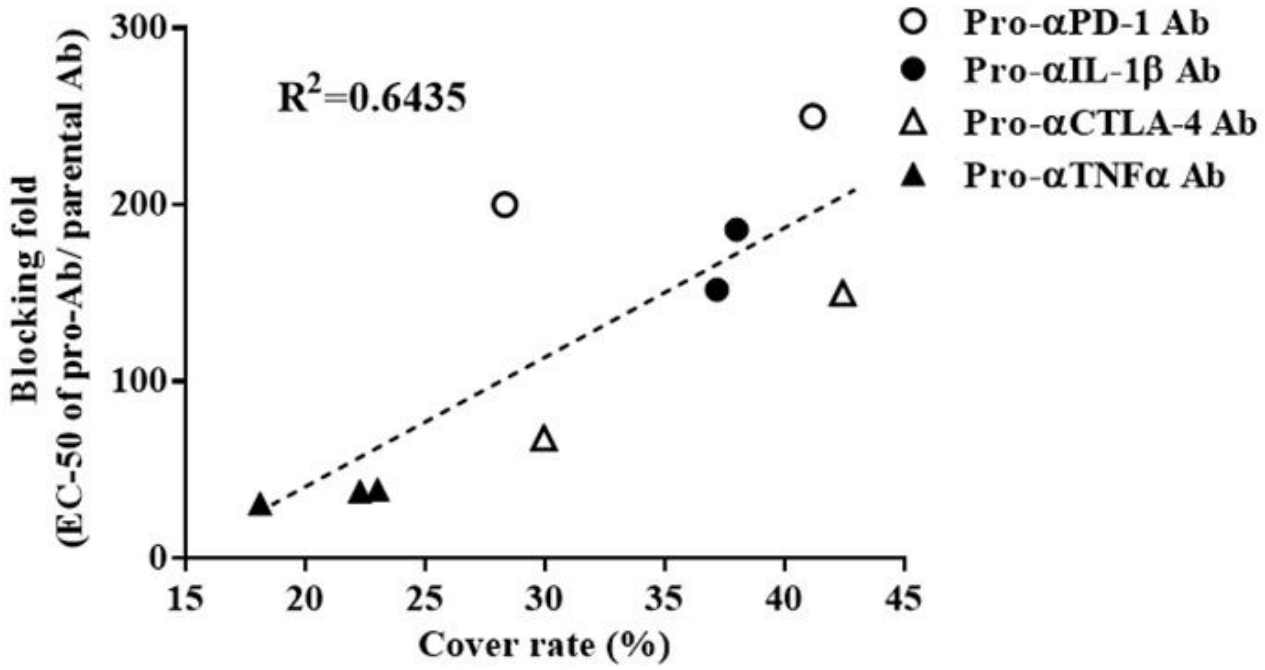

Figure 1

Correlation between blocking fold and cover rate of the different pro-Abs. The correlation between the computer-simulated cover rate and blocking fold was analyzed by GraphPad Prism. We collected the results of pro-αCTLA-4 Ab with L1 and L2 linker (Δ), pro-αPD-1 Ab with L2 and L3 linker (●), pro-αIL-1β Ab with L3 and L4 linker (●) , and pro-αTNFα Ab with L5, L6 and L7 linker (▲), which indicated the positive correlation and the R2 value was 0.6435. The X-axis represents the percentage of cover rate, and the Y-axis represents the blocking fold that is calculated by the EC-50 of pro-Ab/parental Ab.

Supplementary Files

This is a list of supplementary files associated with this preprint. Click to download.

- Graphicalabstract.doc